

# Comparison of Methyl Rotation Axis Order Parameters Derived from Model-Free Analyses of $^2\text{H}$ and $^{13}\text{C}$ Longitudinal and Transverse Relaxation Rates Measured in the Same Protein Sample

Rieko Ishima,<sup>†</sup> Aneta, P. Petkova,<sup>‡</sup> John M. Louis,<sup>‡</sup> and Dennis A. Torchia<sup>\*,†</sup>

Contribution from the Molecular Structural Biology Unit, National Institute of Dental and Craniofacial Research, and the Laboratory of Chemical Physics, National Institutes of Diabetes and Digestive and Kidney Diseases, National Institutes of Health, Bethesda, Maryland 20892

Received February 21, 2001. Revised Manuscript Received April 24, 2001

**Abstract:** Recombinant HIV-1 protease was obtained from bacteria grown on a 98%  $\text{D}_2\text{O}$  medium containing 3- $^{13}\text{C}$  pyruvic acid as the sole source of  $^{13}\text{C}$  and  $^1\text{H}$ . The purified protein is highly deuterated at non-methyl carbons, but contains significant populations of  $^{13}\text{CHD}_2$  and  $^{13}\text{CH}_2\text{D}$  methyl isotopomers. This pattern of isotope labeling permitted measurements of  $^1\text{H}$  and  $^{13}\text{C}$  relaxation rates of  $^{13}\text{CHD}_2$  isotopomers and  $^2\text{H}$  (D) relaxation rates of  $^{13}\text{CH}_2\text{D}$  isotopomers using a single sample. The order parameters  $S_{\text{axis}}^2$ , which characterize the motions of the methyl rotation axes, were derived from model-free analyses of  $R_1$  and  $R_2$  data sets measured for  $^{13}\text{C}$  and  $^2\text{H}$  spins. Our primary goal was to compare the  $S_{\text{axis}}^2$  values derived from the two independent types of data sets to test our understanding of the relaxation mechanisms involved. However,  $S_{\text{axis}}^2$  values derived from the analyses depend strongly on the geometry of the methyl group, the sizes of the quadrupolar and dipolar couplings, and the effects of bond vibrations and librations on these couplings. Therefore uncertainties in these basic physical parameters complicate comparison of the order parameters. This problem was circumvented by using an experimental relationship, between the methyl quadrupolar,  $^{13}\text{C}$ – $^{13}\text{C}$  and  $^{13}\text{C}$ – $^1\text{H}$  dipolar couplings, derived from independent measurements of residual static couplings of weakly aligned proteins by Ottiger and Bax (*J. Am. Chem. Soc.* **1999**, *121*, 4690–4695) and Mittermaier and Kay (*J. Am. Chem. Soc.* **1999**, *121*, 10608–10613). This approach placed a tight experimental restraint on the values of the  $^2\text{H}$  quadrupolar and  $^{13}\text{C}$ – $^1\text{H}$  dipolar interactions and greatly facilitated the accurate comparison of the relative values of the order parameters. When applied to our data this approach yielded satisfactory agreement between the  $S_{\text{axis}}^2$  values derived from the  $^{13}\text{C}$  and  $^2\text{H}$  data sets.

## Introduction

Advances in NMR instrumentation, assignment methodology, and isotope labeling techniques have enabled  $^1\text{H}$ ,  $^2\text{H}$ ,  $^{13}\text{C}$ , and  $^{15}\text{N}$  spin relaxation times to be accurately measured at numerous sequentially assigned sites in proteins. Backbone dynamics has been most commonly studied at amide sites because  $^{15}\text{N}$  isotope enrichment is inexpensive and simple, and model-free analysis of the data affords information about the flexibility of the entire protein backbone in a relatively straightforward manner.<sup>1,2</sup>

Although  $^1\text{H}$ – $^{13}\text{C}$  heteronuclear pulse methodology can easily monitor  $^{13}\text{C}$  spin relaxation of 99%  $^{13}\text{C}$  labeled aliphatic side chains, interpretation of the data is complicated by  $^{13}\text{C}$ – $^{13}\text{C}$  dipolar and  $J$  couplings and by multiexponential decay caused by  $^{13}\text{C}$ – $^1\text{H}$  dipolar cross-correlation.<sup>3</sup> For example, the order parameters of Ala  $\text{CH}_3$  sites in staphylococcal nuclease<sup>4</sup> are

unaccountably small,<sup>5</sup> presumably because  $^{13}\text{C}^1\text{H}_3$  dipolar cross-correlation caused an underestimate of the  $^{13}\text{C}$   $R_2$ .<sup>6</sup> A labeling strategy has been described<sup>7,8</sup> that overcomes these problems by high  $^{13}\text{C}$  enrichment at alternating carbon positions and 50% random perdeuteration. However, this approach requires that a specially modified strain of *E. coli* be used to label the protein of interest. Alternatively, hydrophobic amino acids can be highly  $^{13}\text{C}$  labeled at their methyl carbons by using 3- $^{13}\text{C}$  labeled pyruvate as the sole carbon source in an M9 culture medium,<sup>9</sup> containing a standard *E. coli* strain, BL21. Although  $^1\text{H}$ – $^{13}\text{C}$  dipolar cross-correlation can complicate methyl  $^{13}\text{CH}_3$  relaxation, calculations show that it has a small effect on methyl  $^{13}\text{C}$   $T_1$  and NOE measurements for typical methyl groups in proteins.<sup>3</sup> The cross-correlation problem has been circumvented by measuring deuterium relaxation of  $\text{CH}_2\text{D}$  methyl isotopomers in uniformly 99%  $^{13}\text{C}$  enriched proteins, using a bacterial growth

\* Address correspondence to this author: dtorchia@dir.nidcr.nih.gov; phone.301-496-5750; fax 301-402-5321.

<sup>†</sup> National Institute of Dental and Craniofacial Research.

<sup>‡</sup> National Institutes of Diabetes and Digestive and Kidney Diseases.

(1) Dayie, K. T.; Wagner, G.; Lefevre, J. F. *Annu. Rev. Phys. Chem.* **1996**, *47*, 243–282.

(2) Palmer, A. G. r. *Curr. Opin. Struct. Biol.* **1997**, *7*, 732–737.

(3) Kay, L. E.; Bull, T. E.; Nicholson, L. K.; Griesinger, C.; Schwalbe, H.; Bax, A.; Torchia, D. A. *J. Magn. Reson.* **1992**, *100*, 538–558.

(4) Nicholson, L. K.; Kay, L. E.; Torchia, D. A. *Protein Dynamics as Studied by Solution NMR Techniques*; Sarkar, S. K., Ed.; Elsevier: Amsterdam, 1996; pp 241–279.

(5) Chatfield, D. C.; Szabo, A.; Brooks, B. R. *J. Am. Chem. Soc.* **1998**, *120*, 5301–5311.

(6) Werbelow, L. G.; Grant, D. M. *Intramolecular Dipolar Relaxation in Multispin Systems*; Waugh, J. A., Ed.; Academic Press, INC: New York, 1997; Vol. 9, pp 190–299.

(7) LeMaster, D. M.; Kushlan, D. M. *J. Am. Chem. Soc.* **1996**, *118*, 9255–9264.

(8) LeMaster, D. M. *J. Am. Chem. Soc.* **1999**, *121*, 1726–1742.

(9) Lee, A. L.; Urbauer, J. L.; Wand, A. J. *J. Biomol. NMR* **1997**, *9*, 437–440.

medium containing 50%  $\text{D}_2\text{O}$ .<sup>10</sup> These labeling approaches have made it possible to extract model-free parameters at many methyl sites in a number of proteins.<sup>11–13</sup> This information is of particular interest because methyl groups are often found at protein–ligand interfaces and within hydrophobic cores. Hence information about methyl conformational fluctuations has the potential to improve our understanding of the interactions that stabilize these structures.

We have used a bacterial growth medium containing 3- $^{13}\text{C}$  labeled pyruvate and 99%  $\text{D}_2\text{O}$  to prepare  $^2\text{H}/^{13}\text{C}$  methyl labeled HIV-1 protease.<sup>14</sup> Proteins derived from bacteria grown in this medium are highly deuterated at non-methyl hydrogen sites. At the same time, these proteins have high contents, 16–33%, of  $\text{CH}_2\text{D}$  and  $\text{CHD}_2$  methyl isotopomers of Ala, Val, Leu, and Ile<sup>15</sup> and only methyl signals are observed in  $^1\text{H}$ – $^{13}\text{C}$  HSQC spectra. This permits us to measure and compare  $^2\text{H}$ ,  $^{13}\text{C}$ , and  $^1\text{H}$  relaxation rates within a single sample:  $\text{CH}_2\text{D}$  isotopomers are selectively detected in  $^2\text{H}$  relaxation experiments while  $\text{CHD}_2$  isotopomers are detected in  $^{13}\text{C}$  and  $^1\text{H}$  relaxation experiments. The pattern of isotope enrichment in the protein has the added advantage that one-bond  $^{13}\text{C}$ – $^{13}\text{C}$  couplings and  $^{13}\text{C}$ – $^1\text{H}$  dipolar cross-correlation are absent.

The goal of this article is to compare the methyl rotation axis order parameter,  $S_{\text{axis}}^2$ , from model-free analyses of  $^2\text{H}$  and  $^{13}\text{C}$   $R_1$  and  $R_2$  ( $R_{1\rho}$ ) methyl relaxation data. We derived  $S_{\text{axis}}^2$  from  $^{13}\text{C}$   $R_1$  and  $R_2$  relaxation data, rather than  $R_1$  and NOE<sup>16</sup> because, as we discuss later,  $S_{\text{axis}}^2$  is almost exclusively determined by  $R_2$  and is insensitive to the details of the fast internal motion. In addition, the uncertainty in the  $S_{\text{axis}}^2$  is comparable to the uncertainty in  $R_2$ , typically a few percent. Based on these comments one might surmise that  $S_{\text{axis}}^2$  derived from  $^2\text{H}$  and  $^{13}\text{C}$   $R_1$  and  $R_2$  data sets would be in close agreement, provided that all relaxation mechanisms are accounted for properly. However, one significant problem has hindered comparisons of  $^2\text{H}$  and  $^{13}\text{C}$  order parameters, namely, they are highly sensitive functions of (a) the methyl  $^2\text{H}$  quadrupolar coupling and the C–H dipolar coupling, (b) the effect of bond vibrations and librations on these couplings, and (c) the angle made by the C–H bond and the methyl rotation axis. We show that recent measurements of residual methyl quadrupolar and dipolar couplings in proteins<sup>17,18</sup> place tight experimental restraints on the values of these basic physical parameters. Using these experimentally constrained physical constants in model-free analyses of  $R_1$  and  $R_2$  data yields  $^{13}\text{C}$  and  $^2\text{H}$  methyl axis order parameters that do not depend on assumptions about either vibrational/librational averaging or the values of bond angles or distances. This has enabled us to substantially reduce the uncertainty in the comparison of order parameters derived from  $^2\text{H}$  and  $^{13}\text{C}$  relaxation data.

(10) Muhandiram, D. R.; Yamazaki, T.; Sykes, B. D.; Kay, L. E. *J. Am. Chem. Soc.* **1995**, *117*, 11536–11544.

(11) Kay, L. E.; Muhandiram, D. R.; Farrow, N. A.; Aubin, Y.; Forman-Kay, J. D. *Biochemistry* **1996**, *35*, 361–368.

(12) Constantine, K. L.; Friedrichs, M. S.; Wittekind, M.; Jamil, H.; Chu, C. H.; Parker, R.; Goldfarb, V.; Mueller, L.; Farmer, B. T., II *Biochemistry* **1998**, *37*, 7965–7980.

(13) Lee, A. L.; Kinneer, S. A.; Wand, A. J. *Nat. Struct. Biol.* **2000**, *7*, 72–77.

(14) Ishima, R.; Louis, J. M.; Torchia, D. A. *J. Am. Chem. Soc.* **1999**, *121*, 11589–11590.

(15) Rosen, M. K.; Gardner, K. H.; Willis, R. C.; Parris, W. E.; Pawson, T.; Kay, L. E. *J. Mol. Biol.* **1996**, *263*, 627–636.

(16) Lee, A. L.; Flynn, P. F.; Wand, A. J. *J. Am. Chem. Soc.* **1999**, *121*, 2891–2902.

(17) Ottiger, M.; Bax, A. *J. Am. Chem. Soc.* **1999**, *121*, 4690–4695.

(18) Mittermaier, M.; Kay, L. E. *J. Am. Chem. Soc.* **1999**, *121*, 10608–10613.

## Theoretical Background

**Expressions for Relaxation Rates and the Model-Free Spectral Density Function.** Deuterium longitudinal ( $R_1$ ) and rotating frame ( $R_{1\rho}$ ) relaxation rates were determined by subtracting the measured value of  $R(\text{C}_z\text{H}_z)$  from  $R(\text{D}_z\text{C}_z\text{H}_z)$  and from  $R(\text{D}_x\text{C}_z\text{H}_z)$ , respectively.<sup>10</sup> Deuterium relaxation is dominated by the quadrupolar mechanism and theoretical expressions for deuterium  $R_1$  and  $R_{1\rho}$  are given by Abragam<sup>19</sup>

$$R_1 = 3Q_c^2[J(\omega_D) + 4J(2\omega_D)]/40 \quad (1)$$

$$R_{1\rho} = 3Q_c^2[3J(0) + 5J(\omega_D) + 2J(2\omega_D)]/80 \quad (2)$$

where  $Q_c = e^2qQ/(h/2\pi)$  is the quadrupolar coupling constant and  $J(\omega)$  is the spectral density function.

The major mechanism of methyl  $^{13}\text{C}$ CHD<sub>2</sub> relaxation is the  $^{13}\text{C}$ – $^1\text{H}$  dipolar interaction. In addition, two  $^{13}\text{C}$ – $^2\text{H}$  dipolar interactions and the  $^{13}\text{C}$  chemical shift anisotropy (CSA) contribute to the CHD<sub>2</sub> methyl  $^{13}\text{C}$  relaxation rates. Theoretical expressions for  $^{13}\text{C}$ CHD<sub>2</sub>  $R_1$  and  $R_{1\rho}$  (or  $R_2$ ) that include contributions from the three mechanisms are

$$R_1 = 0.1d_{\text{CH}}^2[3J(\omega_C) + J(\omega_H - \omega_C) + 6J(\omega_C + \omega_H)] + 0.2d_{\text{CD}}^2[3J(\omega_C) + J(\omega_D - \omega_C) + 6J(\omega_C + \omega_D)] + c^2J(\omega_C) \quad (3)$$

$$R_2 = 0.05d_{\text{CH}}^2[4J(0) + 3J(\omega_C) + J(\omega_H - \omega_C) + 6J(\omega_H) + 6J(\omega_C + \omega_H)] + 0.1d_{\text{CD}}^2[4J(0) + 3J(\omega_C) + J(\omega_D - \omega_C) + 6J(\omega_D) + 6J(\omega_C + \omega_D)] + (c^2/6)[3J(\omega_C) + 4J(0)] \quad (4)$$

where,  $d_{\text{CH}}^2 = \gamma_{\text{H}}^2\gamma_{\text{C}}^2h^2/(r_{\text{CH}}^32\pi)^2$ ,  $d_{\text{CD}}^2 = (8/3)\gamma_{\text{D}}^2\gamma_{\text{C}}^2h^2/(r_{\text{CD}}^32\pi)^2$ ,  $\chi^2 = (2/15)(\omega_C\Delta\sigma_C)^2$ , and  $\Delta\sigma_C$  is the methyl  $^{13}\text{C}$  CSA (equal to  $1.5\sigma_{zz} = \sigma_{\parallel} - \sigma_{\perp}$ , for an axially symmetric interaction, where  $\sigma_{zz}$  is the traceless component of the chemical shift tensor).<sup>19</sup> In these equations  $d_{\text{CH}}$ ,  $d_{\text{CD}}$ , and  $Q_c$  denote the dipolar and quadrupolar coupling constants derived from alignment experiments<sup>17,18</sup> that are averaged by high-frequency vibrations and librations.<sup>20,21</sup> Also, note that in eq 4 both  $J(\omega_H)$  and  $J(\omega_D)$  are multiplied by a factor of 6 because transverse cross relaxation<sup>22</sup> is efficient in the effective fields ( $>2J_{\text{CH}}$ ) used in our CPMG and spin lock experiments. Equations 3 and 4 are valid when cross-correlation among the various relaxation mechanisms is either suppressed or small. Our pulse sequences suppress cross-correlation of  $^{13}\text{C}$ – $^1\text{H}/^{13}\text{C}$ – $^2\text{H}$  and  $^{13}\text{C}$ – $^1\text{H}/\text{CSA}$  relaxation mechanisms. Although cross-correlation of the pair of  $^{13}\text{C}$ – $^2\text{H}/^{13}\text{C}$ – $^2\text{H}$  dipolar interactions is not actively suppressed by the pulse sequences, it is strongly attenuated by the  $^2\text{H}$   $R_1$ , ca. 20–25  $\text{s}^{-1}$ , which is over an order of magnitude greater than the  $^{13}\text{C}$  relaxation rates due to the  $^{13}\text{C}$ – $^2\text{H}$  dipolar interactions. Even without this suppression by  $^2\text{H}$  spin flips, the effect of the  $^{13}\text{C}$ – $^2\text{H}/^{13}\text{C}$ – $^2\text{H}$  cross-correlation is small because the  $^{13}\text{C}$ – $^2\text{H}$  dipolar interactions make a minor contribution to  $^{13}\text{C}$  relaxation.

In our calculations of  $^{13}\text{C}$  relaxation rates, we have assumed that  $r_{\text{CH}}$  and  $r_{\text{CD}}$  are the same, because vibrationally averaged CH and CD bond lengths in methane differ by only 0.0002 Å.<sup>23</sup> In addition, we have assumed that the CH bond angles in  $\text{CH}_3$

(19) Abragam, A. *Principles of Nuclear Magnetism*; Oxford University Press: Oxford, 1961.

(20) Henry, E. R.; Szabo, A. *J. Chem. Phys.* **1985**, *82*, 4753–4761.

(21) Case, D. A. *J. Biomol. NMR* **1999**, *15*, 95–102.

(22) Goldman, M. J. *Magn. Reson.* **1984**, *60*, 437–452.

(23) Kuchitsu, K.; Bartell, L. S. *J. Chem. Phys.* **1962**, *36*, 2470–2481.

and CHD<sub>2</sub> isotopomers are the same, because a careful analysis of <sup>1</sup>H and <sup>2</sup>H anisotropic couplings in methane and its deuterated analogues dissolved in nematic liquid crystals showed no difference in CH and CD bond angles.<sup>24</sup> Small deviations in tetrahedral symmetry of mixed H/D methane isotopomers were accounted for by the aforementioned small differences in CH and CD bond lengths.

At 500 MHz the <sup>13</sup>C–<sup>1</sup>H dipolar interaction accounts for about 80% of the transverse relaxation while the relaxation due to the two <sup>13</sup>C–<sup>2</sup>H dipolar interactions and the <sup>13</sup>C CSA (assumed to be ca. 25 ppm) accounts for 12–18% and 3–7%, respectively. The precise contribution of each mechanism depends on the values of the amplitudes and correlation times of the internal and overall motions. The protein sample is highly deuterated, and dipolar relaxation due to nonbonded (“external”) protons and deuterons (H<sup>ext</sup> and D<sup>ext</sup>) is small, but not negligible for <sup>13</sup>C transverse relaxation. Rapid methyl rotation decreases the <sup>13</sup>C transverse relaxation rate by 9-fold, magnifying the relative contributions of C<sup>methyl</sup>–H<sup>ext</sup> and C<sup>methyl</sup>–D<sup>ext</sup> dipolar interactions to R<sub>2</sub>. Although the protein is highly deuterated at non-methyl positions, about 50% of the hydrogen nuclei of the methyl groups are protons, and the protease is bound to a cyclic urea inhibitor, DMP323 (MW ca. 600),<sup>25</sup> which is protonated. Summing the dipolar interactions between various nearby external <sup>1</sup>H and <sup>2</sup>H spins and the methyl carbons using the X-ray coordinates of the protease/DMP323 complex,<sup>25</sup> we estimate that ca. 7% of the <sup>13</sup>C R<sub>2</sub> is due to the external spins. In our application of the model-free approach we have therefore multiplied our measured <sup>13</sup>C R<sub>2</sub> values by 0.93 to compensate for the fact that relaxation by external spins is not included in our calculations. Unlike R<sub>2</sub>, R<sub>1</sub> is not significantly attenuated by methyl rotation unless the rotation rate is very rapid, i.e., τ<sub>rot</sub> < 25 ps. Therefore, the relative contribution of external spin relaxation is nearly 10-fold smaller for R<sub>1</sub> than for R<sub>2</sub>, and can be neglected.

In accordance with the model-free approach, the spectral density functions in eqs 3 and 4 are expressed in terms of the generalized order parameter, S, and correlation times for overall and internal motion according to

$$J(\omega) = S^2 \tau_M / (1 + \omega^2 \tau_M^2) + (1 - S^2) \tau_i / (1 + \omega^2 \tau_i^2) \quad (5)$$

In eq 5, τ<sub>i</sub><sup>-1</sup> = τ<sub>M</sub><sup>-1</sup> + τ<sub>e</sub><sup>-1</sup>, where τ<sub>M</sub> is the correlation time for overall molecular tumbling and τ<sub>e</sub> is an effective internal correlation time. Equation 5 is valid for fast internal motions, i.e., τ<sub>e</sub> ≪ τ<sub>M</sub>. Under this assumption, the order parameter for methyl CH dipolar relaxation can be written as S<sup>2</sup> = S<sub>axis</sub><sup>2</sup> S<sub>Hrot</sub><sup>2</sup>, where S<sub>Hrot</sub> = P<sub>2</sub>(cosθ<sub>H</sub>)<sup>26</sup> for a methyl group whose rotational motion is axially symmetric. S<sub>axis</sub><sup>2</sup> is the order parameter of the methyl rotation axis and θ<sub>H</sub> is the angle made by the methyl rotation axis and the CH bond. The same relations, with H replaced by D, apply for methyl <sup>13</sup>C–<sup>2</sup>H dipolar relaxation and for methyl <sup>2</sup>H quadrupolar relaxation. For a tetrahedral methyl group, θ = 109.47° and S<sup>2</sup> = S<sub>axis</sub><sup>2</sup>/9. Note that S<sup>2</sup> is independent of vibrational/librational motions, because as we have noted, the effects of bond vibrations and librations are included in the experimental values<sup>17,18</sup> of d<sub>CH</sub> and Q<sub>c</sub>. Hence one advantage of our approach is that possible differences in CH vs CD

vibrations/librations are accounted for by our use of the experimentally determined quantities d<sub>CH</sub> and Q<sub>c</sub>.

It should be noted that, unlike the order parameters for the quadrupolar, <sup>13</sup>C–<sup>1</sup>H dipolar and <sup>13</sup>C–<sup>2</sup>H dipolar interactions, the order parameter for the methyl <sup>13</sup>C CSA is not affected by methyl rotation. This can be seen by noting that the 3-fold symmetric C–H bonds in the methyl group make an axially symmetric contribution to the CSA tensor in the case of a static methyl group. Symmetry also requires that methyl rotation is axially symmetric (3-fold or higher symmetry) and it therefore cannot affect the static chemical shift tensor. (Strictly speaking, the CHD<sub>2</sub> isotopomer lacks 3-fold symmetry; however, the H/D isotope effect on the <sup>13</sup>C CSA should be small.) Therefore, for relaxation due to the CSA mechanism, S<sup>2</sup> does not contain the factor S<sub>rot</sub><sup>2</sup> as is the case for the quadrupolar and dipolar mechanisms. This implies that τ<sub>e</sub> in eq 5 may have different values for CSA and dipolar relaxation.

Fortunately because the CSA contribution to relaxation is small at 500 MHz, this distinction between CSA and dipolar τ<sub>e</sub> values can be neglected with little error. Numerical calculations show that the <sup>13</sup>C R<sub>1</sub> and R<sub>2</sub> values change by less than 3% as τ<sub>e</sub><sup>CSA</sup> varies from 1 ps to 2 ns. This statement applies for all values of S<sub>axis</sub><sup>2</sup> and τ<sub>e</sub><sup>dipolar</sup> in the ranges 0.15 < S<sub>axis</sub><sup>2</sup> < 1.0 and 20 ps < τ<sub>e</sub><sup>dipolar</sup> < 2 ns, respectively. For this reason we have derived model-free parameters S<sup>2</sup> and τ<sub>e</sub> from carbon's relaxation data assuming that τ<sub>e</sub> = τ<sub>e</sub><sup>dipolar</sup> = τ<sub>e</sub><sup>CSA</sup>.

**Parameters Used in the Model-Free Analysis.** <sup>15</sup>N relaxation experiments have shown that τ<sub>M</sub> = 11.8 ns for the HIV-1 protease/DMP323 complex dissolved in 94% H<sub>2</sub>O at 20 °C.<sup>27</sup> For our current analysis in the more viscous solvent, 98% D<sub>2</sub>O, we used a 20% larger value, τ<sub>M</sub> = 14.16 ns.<sup>27,28</sup> Inspection of eqs 1–5 shows that, to determine S<sub>axis</sub><sup>2</sup> from <sup>2</sup>H and <sup>13</sup>C R<sub>1</sub> and R<sub>2</sub> measurements, S<sub>Drot</sub>, Q<sub>c</sub>, S<sub>Hrot</sub>, and d<sub>CH</sub> must be known. Because we are interested in comparing the relative values of model-free parameters, we are particularly interested in the ratio S<sub>Hrot</sub>d<sub>CH</sub>/S<sub>Drot</sub>Q<sub>c</sub>. We obtain this quantity from recent measurements of D<sub>CH</sub>/D<sub>CC</sub><sup>17</sup> and ν<sub>Q</sub>/D<sub>CC</sub><sup>18</sup> for methyl groups in weakly aligned proteins, where ν<sub>Q</sub>, D<sub>CH</sub>, and D<sub>CC</sub> are the residual quadrupolar, methyl CH dipolar, and C–C<sup>methyl</sup> dipolar couplings, respectively. As shown by<sup>17,18</sup>

$$S_{Drot}Q_c = -(4/3)(\nu_Q/D_{CC})(\gamma_C^2 h / (r_{CC}^3 2\pi)) \quad (6)$$

$$S_{Hrot}d_{CH} = (D_{CH}/D_{CC})(\gamma_C^2 h / (r_{CC}^3 2\pi)) \quad (7)$$

Note that S<sub>axis</sub> does not enter these equations because the motion of the methyl rotation axis has the same effect on ν<sub>Q</sub> and D<sub>CC</sub>, and also on d<sub>CH</sub> and D<sub>CC</sub>.<sup>17,18</sup> Therefore motion of the methyl rotation axis does not affect either (ν<sub>Q</sub>/D<sub>CC</sub>) or (D<sub>CH</sub>/D<sub>CC</sub>). In addition, the averaging effects of high-frequency methyl <sup>13</sup>C–<sup>1</sup>H and <sup>13</sup>C–<sup>2</sup>H bond vibrations and librations are incorporated into the measured values of ν<sub>Q</sub> and D<sub>CH</sub> and therefore into Q<sub>c</sub> and d<sub>CH</sub>. Using the experimentally determined values (D<sub>CH</sub>/D<sub>CC</sub>) = -3.17<sup>17</sup> and (ν<sub>Q</sub>/D<sub>CC</sub>) = 19.2<sup>18</sup> we find that

$$S_{Drot}Q_c = -25.6(\gamma_C^2 h / (r_{CC}^3 2\pi)) \quad (8)$$

$$S_{Hrot}d_{CH} = -3.17 / (\gamma_C^2 h / (r_{CC}^3 2\pi)) \quad (9)$$

Note that while the values of S<sub>Drot</sub>Q<sub>c</sub> and S<sub>Hrot</sub>d<sub>CH</sub> depend on

(27) Ishima, R.; Louis, J. M.; Torchia, D. A. *J. Mol. Biol.* **2001**, *305*, 515–521.

(28) Lee, L. K.; Rance, M.; Chazin, W. J.; Palmer, A. G. *J. Biomol. NMR* **1997**, *9*, 287–298.

(24) Burnell, E. E.; de Lange, C. A. *J. Chem. Phys.* **1982**, *76*, 3474–3479.

(25) Ala, P.; DeLoskey, R. J.; Huston, E. E.; Jadhav, P. K.; Lam, P. Y. S.; Eyermann, C. J.; Hodge, C. N.; Schadt, M. C.; Lewandowski, F. A.; Weber, P. C.; McCabe, D. D.; Duke, L. J.; Chang, C.-H. *J. Biol. Chem.* **1998**, *273*, 12325–12331.

(26) Lipari, G.; Szabo, A. *J. Am. Chem. Soc.* **1982**, *104*, 4559–4570.



$r_{\text{CC}}$  their ratio does not, and according to eqs 8 and 9 it is given by

$$S_{\text{Hrot}}d_{\text{CH}}/S_{\text{Drot}}Q_{\text{c}} = 0.1238 \quad (10)$$

Hence, although we use  $r_{\text{CC}} = 1.517 \text{ \AA}^{29}$  in our numerical calculation, the relative values of model-free parameters derived from the  $^2\text{H}$  and  $^{13}\text{C}$  relaxation data are independent of our choice of  $r_{\text{CC}}$  as long as  $S_{\text{Hrot}}d_{\text{CH}}$  and  $S_{\text{Drot}}Q_{\text{c}}$  satisfy the ratio given in eq 10. In addition, we note that Ottiger and Bax<sup>17</sup> and Mittermaier and Kay<sup>18</sup> show that  $S_{\text{Hrot}}d_{\text{CH}}$  and  $S_{\text{Drot}}Q_{\text{c}}$  are themselves remarkably constant, from one methyl site to the next, each product varying by an average of ca. 1%. This implies that the quadrupole and dipolar coupling constants are themselves nearly constant, or vary in concert with  $S_{\text{Hrot}}$  and  $S_{\text{Drot}}$  to maintain constant products  $S_{\text{Hrot}}d_{\text{CH}}$  and  $S_{\text{Drot}}Q_{\text{c}}$ .

To obtain explicit numerical values of  $S_{\text{axis}}^2$  the values  $\theta_{\text{H}}$  and  $\theta_{\text{D}}$  must be specified. Although it is not immediately obvious, an advantage of our approach is that the values  $S_{\text{axis}}^2$  derived from model-free analyses of  $R_1$  and  $R_2$  data are not sensitive to the values used for  $\theta_{\text{H}}$  and  $\theta_{\text{D}}$ . This assertion is demonstrated below, both by numerical calculation and by theoretical considerations. Equations 8 and 9 show that the natural choice,<sup>18</sup>  $\theta_{\text{D}} = \theta_{\text{H}} = 109.47^\circ$ , corresponding to tetrahedral methyl geometry, yields  $Q_{\text{c}} = 166.8 \text{ kHz}$ ,  $d_{\text{CH}} = 20.65 \text{ kHz}$ , and  $r_{\text{CH}} = 1.135 \text{ \AA}$ . As noted previously<sup>17</sup> a more reasonable value of  $r_{\text{CH}}$  is obtained using a slightly larger value of  $\theta_{\text{H}}$ . Using eq 9 and  $\theta_{\text{H}} = 110.5^\circ$  one finds  $r_{\text{CH}} = 1.115 \text{ \AA}$ , in agreement with Henry and Szabo<sup>20</sup> and Case.<sup>21</sup> Note that both sets of  $\theta_{\text{H}}$  and  $r_{\text{CH}}$  values satisfy the experimental constraints given in eqs 9 and 10. We will therefore discuss the results of model-free analyses carried out using  $\theta_{\text{H}}$  equal to  $109.47^\circ$  and to  $110.5^\circ$ .

As noted earlier, the  $^{13}\text{C}$  methyl CSA interaction is unaffected by axially symmetric methyl rotation. In addition, unlike the  $^2\text{H}$  quadrupolar and  $^{13}\text{C}^1\text{H}$  dipolar interactions, the methyl CSA tensor is asymmetric because it is significantly influenced by the nonsymmetric external environment of the methyl group. In amino acids<sup>30</sup> and peptides (see Experimental Section), the mean and standard deviations of Leu, Val, and Ile $^{\gamma 2}$  methyl  $\Delta\sigma_{\text{c}}$  and asymmetry parameters,  $\eta$ , are  $25 \pm 5 \text{ ppm}$  and  $0.42 \pm 0.3$ , respectively (recall from eq 3,  $\Delta\sigma_{\text{c}} = 1.5\sigma_{\text{zz}}$  and  $\eta = (\sigma_{\text{yy}} - \sigma_{\text{xx}})/\sigma_{\text{zz}}$ ). Experiment evidence<sup>31,32</sup> indicates that the most shielded and largest component of the methyl tensor lies along the C–C<sup>methyl</sup> bond axis, and we have assumed an axially symmetric chemical shift tensor with  $1.5\sigma_{\text{zz}} = \Delta\sigma_{\text{c}} = 25 \text{ ppm}$  in our model-free analysis.

Although we would prefer to include the contribution of the asymmetric CSA component we see no reliable way to do so. The asymmetric CSA component changes both in magnitude and orientation (in the molecular frame) as the flexible methyl group samples different environments. We are not aware of a means to measure or calculate these changes in the asymmetric CSA component, and for this reason neglect them. Fortunately the total contribution of the axially symmetric CSA component to methyl  $R_1$  and  $R_2$  relaxation is typically less than 7%, at 500 MHz, for a wide range of order parameters and internal correlation times. Therefore, neglecting the contribution of the smaller asymmetric CSA tensor component is expected to

introduce uncertainties of only a few percent in the derived model-free parameters.

## Experimental Section

All solution spectra were recorded on 500 MHz spectrometers using a single sample of HIV-1 protease bound to the potent inhibitor, DMP323, at  $20^\circ\text{C}$  and at a protein concentration of 0.6 mM. The  $^{13}\text{C}$  and  $^2\text{H}$  relaxation data were recorded on Bruker DMX and Varian Inova spectrometers at the NIH and University of Toronto, respectively. The protein was expressed using a medium containing protonated 3- $^{13}\text{C}$  pyruvate in 98%  $\text{D}_2\text{O}$ . Details regarding sample preparation are given by Ishima et al.<sup>14,27</sup>  $\text{H}_2\text{C}_2\text{D}_2$  relaxation rates<sup>10</sup> were measured with relaxation delay times of 0.00082, 0.0042, 0.0087, 0.0137, 0.0193, 0.0255, 0.0327, 0.0411, and 0.0511 s.  $\text{H}_2\text{C}_2\text{D}_2$  relaxation rates were measured with relaxation delay times of 0.0002, 0.00082, 0.00172, 0.0027, 0.0038, 0.00503, 0.0042, 0.00805, and 0.01 s.  $\text{H}_2\text{C}_2$  relaxation rates were measured with relaxation delay times of 0.01, 0.02, 0.04, 0.06, 0.08, and 0.1 s. A total recycle delay of 2–3 s was used for deuterium experiments. Carbon transverse relaxation rates ( $^{13}\text{C}$   $R_{1\rho}$  or  $R_2$ ), at three effective field strengths, 2 kHz, 551 Hz, and 276 Hz, were measured as described.<sup>14</sup> Carbon longitudinal relaxation rates ( $^{13}\text{C}$   $R_1$ ) were measured using relaxation delay times of 0.0313, 0.16313, 0.3213, 0.6413, 0.9613, and 1.2813 s, and with a total recycle delay of 2.4 s. Carbon  $R_{1\rho}$  values were corrected for off-resonance effects as described previously.<sup>14</sup> Proton  $R_2$  experiments were recorded using a pulse sequence similar to that used to measure  $^{13}\text{C}$   $R_2$  but with a relaxation delay prior to the first inept period. In the  $^1\text{H}$   $R_2$  experiments, relaxation delays were 16, 32, 48, 64, 80, and 112 ms. Relaxation data were fit to a single-exponential decay function  $I = I_0\exp(-tR_2)$ . Errors in  $R_1$  and  $R_2$  were derived from Monte Carlo simulations of the decay curves.<sup>33</sup> The average errors in relaxation rates are 2.9% and 2.4% for  $^{13}\text{C}$   $R_1$  and  $R_2$ , 3.3% and 2.5% for  $^2\text{H}$   $R_1$  and  $R_2$ , and 4.6% for  $^1\text{H}$   $R_2$ . The  $^{13}\text{C}$  and  $^2\text{H}$  relaxation times used to derive model-free parameters are tabulated in Supporting Information (supplementary Tables 2 and 3).

The best fit model-free parameters were found by minimizing  $\chi^2 = \{(R_1^{\text{exp}} - R_1^{\text{cal}})/R_1^{\text{error}}\}^2 + \{(R_2^{\text{exp}} - R_2^{\text{cal}})/R_2^{\text{error}}\}^2$  using the simplex minimization package of Matlab (The MathWorks Inc, USA).  $^2\text{H}$  and  $^{13}\text{C}$   $R_2$  values used to derive model-free parameters were measured using a spin lock field of 1 and 2 kHz, respectively. Errors in the model-free parameters were obtained from 200 Monte Carlo simulations. The average errors in  $S_{\text{axis}}^2$ , derived from the  $^2\text{H}$  and  $^{13}\text{C}$  data sets, were 3.0 and 2.9%, respectively. The model-free parameters derived from the  $^{13}\text{C}$  and  $^2\text{H}$  relaxation times are tabulated in the Supporting Information (supplementary Tables 4 and 5).

Methyl  $^{13}\text{C}$  CSA principal values were determined from 1-dimensional  $^{13}\text{C}$  NMR spectra of unlabeled model peptides (Gly-Val-HCl, Gly-Leu-Gly-HCl, and Gly-Ile) in polycrystalline form. The spectra were recorded at room temperature and at a  $^{13}\text{C}$  NMR frequency of 100.4 MHz using standard cross-polarization from  $^1\text{H}$  to  $^{13}\text{C}$  and high-power  $^1\text{H}$  decoupling. Principal values were determined from  $^{13}\text{C}$  spinning sideband intensities in spectra obtained at magic-angle spinning (MAS) frequencies ranging from 600 to 1150 Hz, using a fitting program based on the Herzfeld–Berger analysis of MAS sidebands.<sup>34</sup> The methyl  $^{13}\text{C}$  CSA principal values and their uncertainties are tabulated in the Supporting Information (supplementary Table 6).

## Results and Discussion

**Comparison of Methyl  $^1\text{H}$ ,  $^2\text{H}$ , and  $^{13}\text{C}$   $R_2$  Values.** Nearly 50% of the 99 amino acid residues in the HIV-protease contain at least one methyl group. We measured relaxation rates of 52 of the 77 methyl groups in each protease monomer. This includes nearly every Ala  $\text{C}^\beta$ , Ile  $\text{C}^{\gamma 2}$ , Val  $\text{C}^{\gamma 1}, \text{C}^{\gamma 2}$ , and Leu  $\text{C}^{\delta 1}, \text{C}^{\delta 2}$  site in the protein. We did not obtain data for Thr  $\text{C}^{\gamma 2}$  and Ile  $\text{C}^{\delta 1}$  methyl groups because they are almost fully deuterated. Although data were acquired for the two highly

(29) Engh, R. A.; Huber, R. *Acta Crystallogr.* **1991**, *A47*, 392–400.

(30) Ye, C.; Fu, R.; Hu, J.; Hou, L.; Ding, S. *Magn. Reson. Chem.* **1993**, *31*, 699–704.

(31) Naito, A.; Ganapathy, S.; Akasaka, K.; McDowell, C. A. *J. Chem. Phys.* **1980**, *74*, 3190–3197.

(32) Harper, J. K.; McGeorge, G.; Grant, D. M. *Magn. Reson. Chem.* **1998**, *36*, S135–S144.

(33) Kamath, U.; Shriver, J. W. *J. Biol. Chem.* **1989**, *264*, 5586–5592.

(34) Herzfeld, J.; Berger, A. E. *J. Chem. Phys.* **1980**, *73*, 6021–6030.

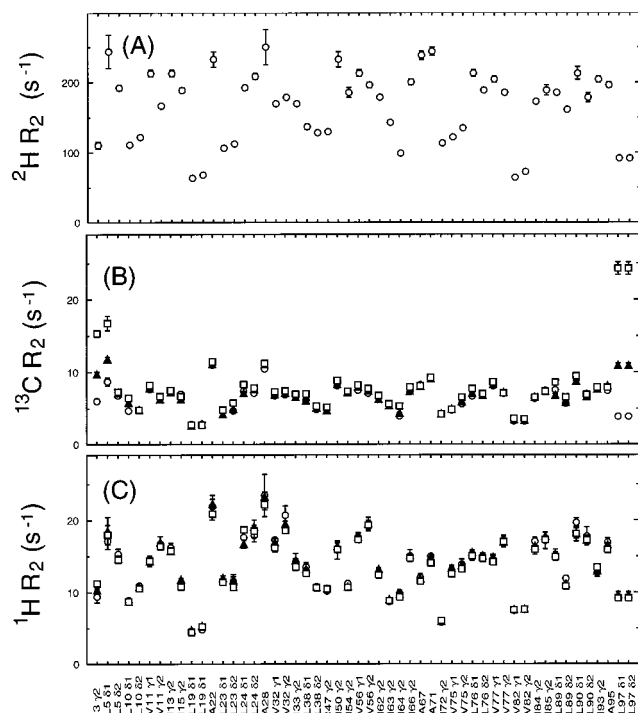


**Figure 1.** (A) Deuterium, (B) carbon, and (C) proton transverse relaxation rates ( $R_2$ ) at various methyl sites in the HIV-1 protease, plotted as a function of the amino acid residue.  $^{13}\text{C}$  and  $^1\text{H}$   $R_2$  were measured at effective field strengths at 2 kHz ( $\circ$ ) using a spin lock and at 551 ( $\blacktriangle$ ) and 276 Hz ( $\square$ ) using a CPMG pulse sequence. The plots show that  $R_2$  varies significantly from one methyl to another, and that chemical exchange contributes to the  $^{13}\text{C}$   $R_2$  at methyl sites in the N- and C-terminus of the protein.

flexible methionine methyl groups, the relaxation rates were so small that they could not be precisely measured using relaxation delays appropriate to the other methyl sites.

A comparison of  $^2\text{H}$ ,  $^{13}\text{C}$ , and  $^1\text{H}$   $R_2$  values, the latter two rates measured at three effective RF fields, Figure 1, shows that  $R_2(^2\text{H}) \gg R_2(^1\text{H}) > R_2(^{13}\text{C})$ . This progression in relaxation rates is expected because (a) the quadrupole interaction is much larger than the  $^1\text{H}$ – $^{13}\text{C}$  dipolar interaction and (b) dipolar relaxation by external protons,  $\text{H}^{\text{ext}}$  (not bonded to the methyl carbon, and primarily in other methyl groups and in DMP323), contribute much more to the methyl  $^1\text{H}$   $R_2$  than to the methyl  $^{13}\text{C}$   $R_2$ . The latter conclusion is a consequence of the 4-fold larger proton magnetogyric ratio and because  $^1\text{H}^{\text{methyl}}$ – $^1\text{H}^{\text{ext}}$  distances are less than  $^{13}\text{C}^{\text{methyl}}$ – $\text{H}^{\text{ext}}$  distances. A significant advantage of the large quadrupole interaction is that it is the only mechanism that contributes to  $^2\text{H}$  relaxation, and this greatly simplifies  $^2\text{H}$  data analysis. In addition, the large quadrupolar coupling and the small  $^2\text{H}$  chemical shift range make the  $^2\text{H}$   $R_2$  totally insensitive to motions on the millisecond to microsecond (chemical exchange) time scale. Clear evidence for such motion is manifest in the RF field dependence of the  $^{13}\text{C}$   $R_2$  values of residues 3, 5, and 97.<sup>27</sup> Unlike the  $^{13}\text{C}$   $R_2$  values, the  $^1\text{H}$   $R_2$  values are unaffected by chemical exchange occurring at these sites, presumably because the methyl proton chemical shifts are much less sensitive to conformation changes (that do not involve changes in ring currents) than the methyl carbons.<sup>35</sup> It may be possible to observe the effect of chemical exchange on the  $^1\text{H}$   $R_2$  at higher external fields or at smaller RF fields using the method of Loria et al.<sup>36</sup>

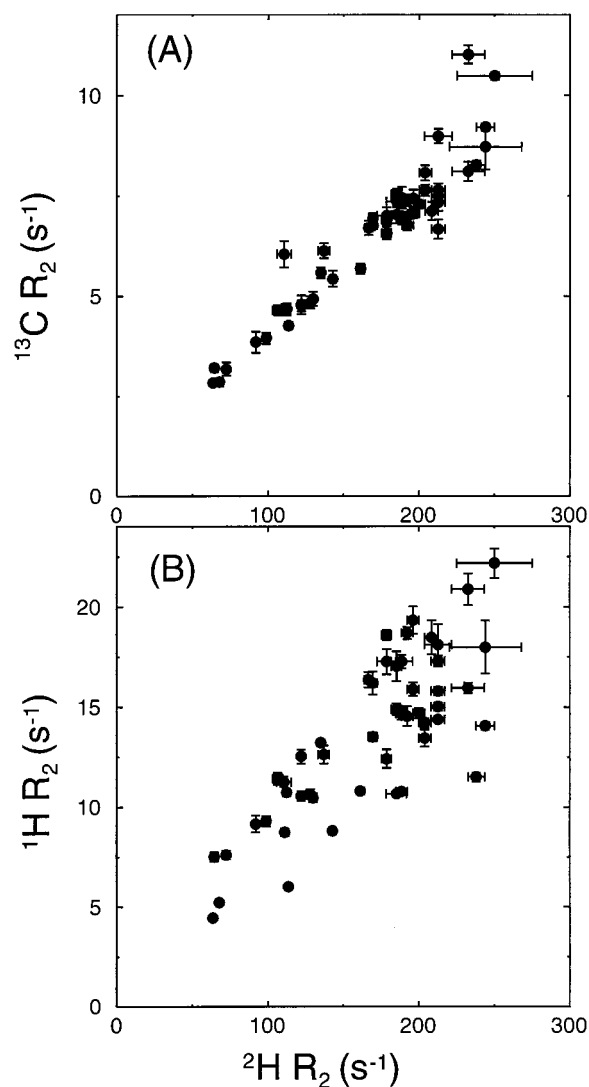


**Figure 2.** Comparison of plots of (A)  $^{13}\text{C}$   $R_2$  versus  $^2\text{H}$   $R_2$  and (B)  $^1\text{H}$   $R_2$  versus  $^2\text{H}$   $R_2$ . As discussed in the text, a better correlation of  $^{13}\text{C}$  and  $^2\text{H}$   $R_2$  values is observed because in both cases interactions responsible for transverse relaxation are parallel to the methyl rotation axis. In all three cases,  $R_2$  was measured using spin-locks with RF field strengths of 2 kHz for  $^{13}\text{C}$  and  $^1\text{H}$  and 1 kHz for  $^2\text{H}$ .

It is clear from Figure 1 that there are substantial variations in the  $^2\text{H}$ ,  $^{13}\text{C}$ , and  $^1\text{H}$   $R_2$  values from one methyl site to another. Figure 2 shows that these variations are well correlated. The correlation coefficient,  $r$ , of the  $^2\text{H}$  and  $^{13}\text{C}$   $R_2$  values is 0.95 at a 2 kHz  $^{13}\text{C}$  spin-lock field, which minimizes chemical exchange contributions to the  $^{13}\text{C}$   $R_2$ . This result is reasonable because, despite their different magnitudes, the  $^{13}\text{C}$ – $^1\text{H}$  dipolar and  $^2\text{H}$  quadrupolar tensors are almost parallel and are therefore scaled in nearly the same fashion by internal motions of the methyl group. Hence the  $J(0)$  spectral density terms that dominate both  $^2\text{H}$  and  $^{13}\text{C}$  transverse relaxation are nearly proportional to one another. It is interesting that, despite contributions from external protons to  $^1\text{H}$   $R_2$  values, the  $^1\text{H}$  and  $^2\text{H}$   $R_2$  values are clearly correlated,  $r = 0.81$  (the probability that the  $R_2$  values are not correlated is  $<10^{-8}$ ). The correlation is not as good as that observed for the  $^{13}\text{C}$  and  $^2\text{H}$   $R_2$  values presumably because the  $^1\text{H}^{\text{methyl}}$ – $^1\text{H}^{\text{ext}}$  dipolar interactions vary considerably from one methyl site to the next.

(35) Wishart, D. S.; Watson, M. S.; Boyko, R. F.; Sykes, B. D. *J. Biomol. NMR* **1997**, *10*, 329–336.

(36) Loria, J. P.; Rance, M.; Palmer, A. G. *J. Am. Chem. Soc.* **1999**, *121*, 2331–2332.

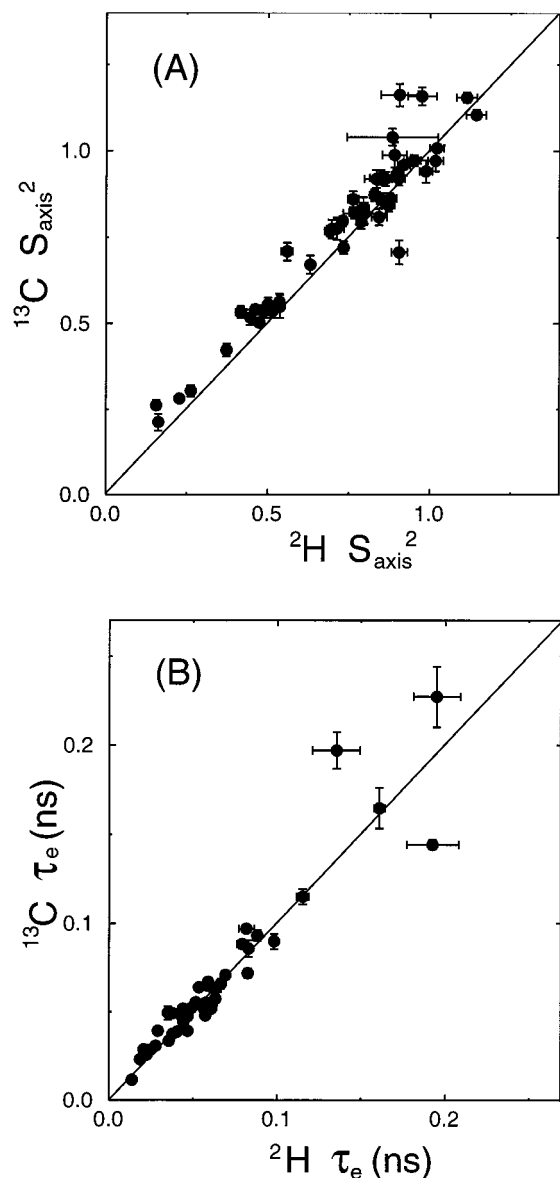


**Figure 3.** Comparison of plots of (A) generalized order parameter,  $S_{\text{axis}}^2$ , determined using  $^{13}\text{C}$   $R_1$  and  $^{13}\text{C}$   $R_2$  data, versus  $S_{\text{axis}}^2$ , determined using  $^2\text{H}$   $R_1$  and  $^2\text{H}$   $R_2$  data and (B) Correlation times for internal motion,  $\tau_e$ , determined using  $^{13}\text{C}$   $R_1$  and  $^{13}\text{C}$   $R_2$  data versus  $\tau_e$  determined using  $^2\text{H}$   $R_1$  and  $^2\text{H}$   $R_2$ . Although the results shown were obtained with  $\theta_D = \theta_H = 109.47^\circ$  the correlation of  $S_{\text{axis}}^2$  displayed in part A is insensitive to small changes in the value of either angle (see text for further discussion).

**Comparison of  $S_{\text{axis}}^2$  Values Derived from  $^2\text{H}$  and  $^{13}\text{C}$  Data.** Values of  $S^2$  and  $\tau_e$  were derived from either  $^2\text{H}$  or  $^{13}\text{C}$   $R_1$  and  $R_2$  data using the model-free spectral density function given in eq 5. The analysis was done for 48 residues whose  $^{13}\text{C}$   $R_2$  values do not contain large chemical exchange contributions (i.e., I3 $\gamma_2$ , L5 $\delta_1$ , L97 $\delta_1$ , and L97 $\delta_2$  were excluded from the analysis, Figure 1B). Values of  $S_{\text{axis}}^2$  were obtained from the relation  $S_{\text{axis}}^2 = S^2/S_{\text{rot}}^2$ , where  $S_{\text{rot}} = P_2(\cos\theta)$  and  $\theta = \theta_H = \theta_D = 109.47^\circ$ . The results presented in Figure 3 show that values of  $S_{\text{axis}}^2$  and  $\tau_e$  determined using  $^{13}\text{C}$  relaxation data are in good agreement with these model-free parameters determined using  $^2\text{H}$  data.

**The Dependence of the Model-Free Parameters upon  $\theta$ .** As we have noted earlier, the values of  $S_{\text{axis}}^2$  derived from the model-free analysis of  $R_1$  and  $R_2$  data are insensitive to the choice of  $\theta$  provided that the parameter relationships specified

in eqs 8–10 are maintained. A model-free analysis of the CHD $_2$   $^{13}\text{C}$  relaxation data, performed using  $\theta_H = 110.5^\circ$  and  $\theta_D = 109.47^\circ$ , yielded  $^{13}\text{C}$   $S_{\text{axis}}^2$  values that differ from those in Figure 3A (where  $\theta_H = 109.45^\circ$ ) by only 1–2%. Therefore the good agreement of model-free parameters derived from  $^{13}\text{C}$  and  $^2\text{H}$  relaxation data is retained when we assume that  $\theta_H = 110.5^\circ$  and  $\theta_D = 109.47^\circ$ . These angles are close to values used by Ottiger and Bax<sup>17</sup> and Mittermaier and Kay,<sup>18</sup> and as noted earlier,  $\theta_H = 110.5^\circ$  yields a more reasonable value of  $r_{\text{CH}}$ , 1.115 Å,<sup>20,21</sup> than does  $\theta_H = 109.47^\circ$ .

In contrast with the insensitivity of  $S_{\text{axis}}^2$  to the choice of  $\theta_H$ , the  $^{13}\text{C}$   $\tau_e$  values obtained assuming  $\theta_H = 110.5$  are about 8% smaller than those in Figure 3B. Insight into the observed dependence of the model-free parameters on  $\theta_H$  is afforded by approximate expression for  $S_{\text{axis}}^2$  and  $\tau_e$  that are obtained from eqs 3–5. At 500 MHz with  $\tau_m = 14.2$  ns,  $30$  ps  $< \tau_e < 100$  ps, and  $\theta_H$  close to  $109.5^\circ$  one obtains the following approximate expression from eqs 3–5

$$R_2 \approx k_{2\text{C}} d_{\text{CH}}^2 S_{\text{Hrot}}^2 S_{\text{axis}}^2 \tau_m \quad (11)$$

$$R_1 \approx k_{1\text{C}} d_{\text{CH}}^2 \tau_e \quad (12)$$

where  $k_{2\text{C}}$  and  $k_{1\text{C}}$  are numerical constants. Although a  $1^\circ$  change in  $\theta_H$  changes  $S_{\text{Hrot}}^2$  by 10%, the product  $d_{\text{CH}}^2 S_{\text{Hrot}}^2$  remains constant according to eq 9. Therefore according to eq 11  $S_{\text{axis}}^2$  is insensitive to small variations in  $\theta_H$ . In contrast, because eq 9 requires that  $d_{\text{CH}}^2 \propto S_{\text{Hrot}}^{-2}$ ,  $\tau_e$  is sensitive to small changes in  $\theta_H$  according to eq 12. Similar remarks apply to model-free parameters derived from  $^2\text{H}$  relaxation data. In agreement with these considerations, plots comparing  $S_{\text{axis}}^2$  and  $\tau_e$  derived from  $^{13}\text{C}$  and  $^2\text{H}$  data assuming that  $\theta_H$  and  $\theta_D = 110.5^\circ$  (data not shown) are nearly identical to Figure 3A,B, except that  $\tau_e$  values derived from both  $^{13}\text{C}$  and  $^2\text{H}$  data are about 8% smaller.

**Other Sources of Uncertainty in  $S_{\text{axis}}^2$ .** Although the  $^{13}\text{C}$  and  $^2\text{H}$  order parameters are well correlated, the average difference in the order parameters is about 2.6 times greater (average  $\chi^2 = 6.9$ , Supporting Information, Table 1) than expected, assuming that errors in  $S_{\text{axis}}^2$  are due solely to random errors (noise) in the relaxation data. The larger than expected  $\chi^2$  values result in part from the fact that the  $^{13}\text{C}$  order parameters are systematically larger than the  $^2\text{H}$  order parameters. Multiplying all  $^{13}\text{C}$  order parameters by 0.95 or reducing them all by 0.04 reduces the average  $\chi^2$  to 4.6 and 3.5, respectively. A possible cause of the systematic difference in the order parameters is that we have underestimated the contribution to  $^{13}\text{C}$  relaxation from either the CSA or the external protons, or both. For example, using  $\Delta\sigma_{\text{C}} = 30$  ppm instead of 25 ppm in the model-free analysis results in a 3–5% decrease in  $^{13}\text{C}$   $S_{\text{axis}}^2$ . The values of  $\Delta\sigma_{\text{C}}$  measured in amino acids and small peptides vary from 15 to 40 ppm, and 25 ppm appears to be a reasonable choice for the average value of  $\Delta\sigma_{\text{C}}$ . However, it is clearly an estimate. We also note that our estimate of an average 7% contribution to  $R_2$  from external spins is derived from the hydrogen coordinates of the crystal structure,<sup>25</sup> and does not take account of side chain mobility.

Chemical exchange,  $R_{\text{ex}}$ , contributions to  $R_2$  could also cause the derived values of  $^{13}\text{C}$   $S_{\text{axis}}^2$  to be overestimated. While we have used RF field dependence to identify and exclude all methyl sites having large  $R_{\text{ex}}$  contributions, it is possible that some sites having small exchange contributions have been included in our analysis. A chemical exchange contribution of  $0.3$  s $^{-1}$  would have little impact on the value of  $^{13}\text{C}$   $S_{\text{axis}}^2$  derived for a  $^{13}\text{C}$  site with a large value of  $R_2$  of ca.  $10$  s $^{-1}$ . However,



a few methyl sites in our data have  $R_2$  values of ca.  $3 \text{ s}^{-1}$ . An  $R_{\text{ex}}$  contribution of ca.  $0.3 \text{ s}^{-1}$  at these sites (which typically have the smallest values of  $S_{\text{axis}}^2$ ) causes  $^{13}\text{C } S_{\text{axis}}^2$  to be overestimated by ca. 10%.

In addition to these systematic uncertainties in the  $^{13}\text{C } S_{\text{axis}}^2$  values, site variations in CSA and external spin relaxation contributions to  $^{13}\text{C}$  relaxation are estimated to cause ca. 3% site variations in derived values of  $^{13}\text{C } S_{\text{axis}}^2$ . The data of Ottiger and Bax<sup>17</sup> and Mittermaier and Kay<sup>18</sup> indicate that the methyl dipolar and quadrupolar interactions have site variations of ca. 1%, and these result in site variations in  $^{13}\text{C } S_{\text{axis}}^2$  and  $^2\text{H } S_{\text{axis}}^2$  of ca. 2%. When we combine these site variations in relaxation parameters with the average 3% uncertainty in  $S_{\text{axis}}^2$  due to random errors, we estimate a total uncertainty of 3.5% in derived values of  $^2\text{H } S_{\text{axis}}^2$  and about 5% in the values of  $^{13}\text{C } S_{\text{axis}}^2$ . These uncertainties in  $^{13}\text{C } S_{\text{axis}}^2$  and  $^2\text{H } S_{\text{axis}}^2$  due to random errors and site-variations in relaxation parameters, together with the ca. 5% systematic uncertainty in  $^{13}\text{C } S_{\text{axis}}^2$  values, account for our observation that the average difference in the  $^{13}\text{C}$  and  $^2\text{H } S_{\text{axis}}^2$  values is ca. 9%.

**The Impact of Anisotropic Overall Motion on the Calculation of Order Parameters.** We have assumed isotropic overall motion in our model-free analyses. However, it has been shown that the protease/DMP323 complex reorients as an axially symmetric rotor with an anisotropy of  $D_{\parallel}/D_{\perp} = 1.35$ .<sup>37</sup> We now estimate the size of the errors in  $^{13}\text{C } S_{\text{axis}}^2$  and  $^2\text{H } S_{\text{axis}}^2$  that are introduced by neglecting anisotropic overall motion. We do this using an approximate expression for the model-free spectral density function of the methyl group attached to an axially symmetric rotor, with  $\epsilon^2 = (D_{\parallel}/D_{\perp} - 1)^2 \ll 1$ . Because the rotational anisotropy is not large, we factor out the internal motion contribution to the correlation function in a manner similar to Lipari and Szabo.<sup>38</sup> In the large molecule limit,  $(\omega\tau_a)^2 \gg 1$ ,  $\tau_a \gg \tau_f$  where  $\tau_a = 1/(4D_{\perp} + 2D_{\parallel})$  is the average overall correlation time of the molecule and  $\tau_f$  is the correlation time for methyl rotation, one obtains the following approximate expression for the order parameter of either a  $^{13}\text{C}$  or  $^2\text{H}$  spin in a methyl group attached to an axially symmetric rotor

$$\underline{S}_{\text{axis}}^2 [1 + (\epsilon/3)P_2(\cos\alpha)] = R_2/R_{20} \quad (13)$$

In this equation,  $R_{20}$  is the transverse relaxation rate that would be observed with a rapidly rotating methyl, having  $S_{\text{axis}}^2 = 1$ , attached to an isotropic rotor having overall correlation time  $\tau_a$ , and  $\alpha$  is the angle made by the methyl rotation axis and the symmetry axis of the molecule. The notation  $\underline{S}_{\text{axis}}^2$  is used to indicate that the order parameter is derived including the effect of anisotropic overall motion. If one assumes isotropic motion, the approximate model-free expression for  $S_{\text{axis}}^2$  is

$$S_{\text{axis}}^2 = R_2/R_{20} \quad (14)$$

Comparison of these equations shows that the axial order parameter obtained from the isotropic analysis is equal to  $\underline{S}_{\text{axis}}^2 [1 + (D_{\parallel}/3D_{\perp})P_2(\cos\alpha)]$ . Hence the value of  $S_{\text{axis}}^2$  derived from the isotropic analysis is correct only if  $\alpha$  is close to the magic angle. For  $\alpha$  ca.  $0^\circ$  the value of  $S_{\text{axis}}^2$  is fractionally overestimated by  $\epsilon/3$ , while for  $\alpha$  ca.  $90^\circ$  it is underestimated by  $\epsilon/6$ . In the case of the protease where  $\epsilon/3 = 0.12$ , the absolute values of  $S_{\text{axis}}^2$  could be in error by as much as +12% or -6%. Note, however, that neglect of anisotropic motion produces the same fraction error in  $S_{\text{axis}}^2$  derived from both  $^{13}\text{C}$  and  $^2\text{H}$

relaxation data, because the dipolar and quadrupolar interaction tensor alignments are nearly parallel. Therefore, our previous remarks regarding the relative values of  $^{13}\text{C } S_{\text{axis}}^2$  and  $^2\text{H } S_{\text{axis}}^2$  need not be modified.

It is interesting that of the four residues (A22, A67, A71, and L90) that have  $S_{\text{axis}}^2$  values significantly larger than unity, Figure 3A, A71 and L90 have values of  $\alpha$  of  $13^\circ$  and  $17^\circ$ , respectively. Our above discussion indicates that the small values of  $\alpha$  for these residues account in large measure for their large values of  $S_{\text{axis}}^2$ . The value of  $\alpha$  is not available for A67 because a Cys residue occupies this position in the sequence of the protease/DMP323 complex whose structure is available. Hence, A22 ( $\alpha = 50^\circ$ ) is the only methyl site for which  $\alpha$  is large and  $S_{\text{axis}}^2$  is significantly greater than unity.

Even after accounting for the effects of anisotropic motion, all four Ala residues have large values of  $S^2$ , as might be expected because of the short length of the Ala side chain. In general, methyl groups in longer side chains that have  $S^2$  greater than ca. 0.8 are buried in the hydrophobic interior of the protein/DMP323 complex, while methyl sites having  $S^2$  below ca. 0.5 are solvent accessible. There are some interesting exceptions to this general statement that are discussed elsewhere.<sup>27</sup>

**Comparison with Methyl Order Parameters Obtained by Other Investigators.** Wand et al.<sup>16</sup> reported that  $^{13}\text{C}$  methyl  $S_{\text{axis}}^2$  values derived using the simple model-free spectral density function, eq 5, differed significantly from those derived from deuterium relaxation data. Their relaxation data consisted of  $^{13}\text{CH}_3 R_1$  and  $^{13}\text{C}-\{\text{H}\}$  NOEs measured at four external fields;  $R_2$  was not measured, to avoid possible complications resulting from  $^{13}\text{CH}_3$  dipolar cross-correlation and chemical exchange. Herein, we observed that  $S_{\text{axis}}^2$  derived from  $^{13}\text{C}(\text{CHD}_2)$  and  $^2\text{H}(\text{CH}_2\text{D}) R_1/R_2$  data sets were in good agreement. LeMaster<sup>8</sup> reported that  $S_{\text{axis}}^2$  values determined by  $^{13}\text{C } R_1/R_2$  data sets systematically differed from those determined using  $^{13}\text{C } R_1/^{13}\text{C}-\{\text{H}\}$  NOE data, but agreed with order parameters obtained when  $R_2$  was included with the  $R_1$  and NOE data.

It is recognized<sup>8,16,39</sup> that these observations stem from the fact that for methyl relaxation  $S_{\text{axis}}^2$  is highly sensitive to  $R_2$  and nearly independent of  $R_1$ . This is clearly shown by eqs 11 and 12. Because  $R_2$  is nearly proportional to  $S_{\text{axis}}^2$  for both  $^2\text{H}$  and  $^{13}\text{C}$  relaxation, the values of  $S_{\text{axis}}^2$  derived from both  $^2\text{H}$  and  $^{13}\text{C } R_1, R_2$  measurements are insensitive to the details of internal motion. Therefore, it is to be expected that similar values of  $S_{\text{axis}}^2$  will be obtained from  $R_1$  and  $R_2$  data sets measured for each nucleus. Although an extended model-free analysis of  $^{13}\text{C } R_1$  and  $^{13}\text{C}-\{\text{H}\}$  NOE data of ubiquitin yielded order parameters in significantly better agreement with those obtained from  $^2\text{H } R_1$  and  $R_2$  data,<sup>16</sup> small uncertainties in methyl  $R_1$  and NOE values result in large uncertainties in  $S_{\text{axis}}^2$ . In addition, because the derived values of  $S_{\text{axis}}^2$  are highly sensitive to the details of the internal motion, the approximate nature of the extended model-free, EMF, spectral density function adds a further source of uncertainty in  $S_{\text{axis}}^2$ .<sup>8,40</sup> Provided that chemical exchange is absent, more robust values of  $S_{\text{axis}}^2$  are obtained from  $^{13}\text{C } R_1$  and  $R_2$  data using the simple model-free function, eq 3, which directly yields  $S_{\text{axis}}^2/(P_2(\cos\theta_m))^2$ .<sup>38</sup> Note that  $\tau_c$  determined using eq 3 cannot generally be associated with a specific internal motion. Information about the time scales of internal motions can be obtained from an EMF analysis of  $^{13}\text{C } R_1, R_2$ , and NOE measurements, ideally measured at multiple fields. Because our primary interest is the comparison of methyl order parameters,

(39) Kay, L. E.; Nicholson, L. K.; Delaglio, F.; Bax, A.; Torchia, D. A. *J. Magn. Reson.* **1992**, *97*, 359–375.

(40) Clore, G. M.; Driscoll, P. C.; Wingfield, P. T.; Gronenborn, A. M. *Biochemistry* **1990**, *29*, 7387–7401.

(37) Tjandra, N.; Wingfield, P.; Stahl, S.; Bax, A. *J. Biomol. NMR* **1996**, *8*, 273–284.

(38) Lipari, G.; Szabo, A. *J. Am. Chem. Soc.* **1982**, *104*, 4546–4559.

and not in investigating the time scales of methyl internal motions, we have not included  $^{13}\text{C}$  NOEs in our analysis.

Wand<sup>16</sup> has thoroughly discussed the relative merits of using multifield  $^{13}\text{C}$   $R_1$ , NOE data compared with  $^2\text{H}$   $R_1$  and  $R_2$  data for deriving model-free parameters. From our perspective,  $^2\text{H}$  relaxation data provide more accurate estimates of  $S_{\text{axis}}^2$  than  $^{13}\text{C}$  relaxation measurements, in the case of moderate sized proteins, MW < 30 kDa. A single mechanism is responsible for  $^2\text{H}$  relaxation, cross-correlation effects are very small,<sup>41</sup> chemical exchange is negligible,  $S_{\text{axis}}^2$  is highly sensitive to  $R_2$ , and  $S_{\text{rot}Q_c}$  is highly uniform. On the other hand, in the case of large proteins, it may be more desirable to derive  $S_{\text{axis}}^2$  from  $^{13}\text{C}$  relaxation data. Extrapolating the protease  $R_2$  data to a protein having  $\tau_M = 30$  ns and  $S_{\text{axis}}^2 = 1$ , we find  $R_2$  ca. 600  $\text{s}^{-1}$  for  $^2\text{H}$  spins. Measurement of such large  $^2\text{H}$   $R_2$  values require the use large  $B_1$  fields and very short relaxation delays. In contrast the  $^{13}\text{C}$  and  $^1\text{H}$   $R_2$  values are estimated to be ca. 15 and 30  $\text{s}^{-1}$ , respectively, and cause no measurement problems. In fact, the increase in the  $^{13}\text{C}$   $R_2$  with molecular weight makes the derived values of  $S_{\text{axis}}^2$  less sensitive to chemical exchange contributions to  $R_2$ .

We note one other aspect of  $^2\text{H}$  relaxation that may be useful. Equations 1 and 2 show that measurements of  $R_1$  and  $R_2$  at two field strengths  $B_0$  and  $2B_0$  will yield  $J(0)$ ,  $J(\omega_D)$ ,  $J(2\omega_D)$ , and  $J(4\omega_D)$ , where  $\omega_D$  is the  $^2\text{H}$  Larmor frequency in field  $B_0$ .  $J(\omega)$  could be obtained at additional frequencies by including  $R_1$  and  $R_2$  measurements obtained at other available field strengths. Therefore, in the event that a model-free analysis is unable to fit multifield  $^2\text{H}$  relaxation data, values of  $J(\omega)$  can be obtained at numerous discrete frequencies that may provide some insight regarding the complex motion of a methyl side chain.

In summary, we find that, within the experimental uncertain-

ties, self-consistent values of model-free parameters are obtained from analyses of methyl  $^{13}\text{C}$  and  $^2\text{H}$   $R_1$  and  $R_2$  relaxation rates. In addition to obtaining good agreement between  $^2\text{H}$  and  $^{13}\text{C}$  derived order parameters, absolute values  $S_{\text{axis}}^2$  are found to be in the physically reasonable range of 0.15 to 1.0. An essential feature of our approach is the use of highly uniform values of  $S_{\text{Drot}Q_c}$  and  $S_{\text{Hrot}d_{\text{CH}}}$  derived from measurements of residual dipolar and quadrupolar couplings.<sup>17,18</sup> Even though small errors remain due to uncertainties in  $^{13}\text{C}$  relaxation due to chemical exchange, external protons, and the  $^{13}\text{C}$  CSA values, the two independent sets of order parameters agree quite well. This suggests that use of quadrupolar and dipolar couplings, derived from alignment experiments, can improve the accuracy of order parameters obtained from model-free analyses of relaxation data.

**Acknowledgment.** We thank Ad Bax, Attila Szabo, Rob Tycko, and James P. Yesinowski for helpful discussions, Frank Delaglio and Daniel S. Garrett for data processing software, and DuPont Pharmaceuticals for DMP323. We thank Lewis E. Kay for helpful discussions and instrument time, enabling us to measure accurate  $^2\text{H}$  relaxation rates, at a time when our spectrometer  $^2\text{H}$  channel malfunctioned. This work was supported by the Intramural AIDS Targeted Anti-Viral Program of the Office of the Director of the National Institutes of Health.

**Supporting Information Available:** One table listing the differences in  $^{13}\text{C}$  and  $^2\text{H}$   $S_{\text{axis}}^2$  values, two tables listing the  $^{13}\text{C}$  and  $^2\text{H}$  relaxation times, two tables listing the  $^{13}\text{C}$  and  $^2\text{H}$  model-free parameters, and one table listing the principal components of the  $^{13}\text{C}$  methyl chemical shift tensors in three model peptides (PDF). This material is available free of charge via the Internet at <http://pubs.acs.org>.

(41) Yang, D.; Kay, L. E. *J. Mol. Biol.* **1996**, *263*, 369–382.